PERGAMON

Deep-Sea Research II 49 (2002) 585–602

DEEP-SEA RESEARCH
PART II

www.elsevier.com/locate/dsr2

Water masses and distribution of physico-chemical properties in the Western Bransfield Strait and Gerlache Strait during Austral summer 1995/96

M.A. García[a,b,*], C.G. Castro[c], A.F. Ríos[c], M.D. Doval[c], G. Rosón[d], D. Gomis[e,f], O. López[g]

[a] *Laboratori d'Enginyeria Marítima, ETS d'Enginyers de Camins, Canals i Ports, Universitat Politècnica de Catalunya, Barcelona, Spain*
[b] *Direcció General de Ports i Transports, Generalitat de Catalunya, Av. Josep Tarradellas 2-6, 08029 Barcelona, Spain*
[c] *Instituto de Investigacions Mariñas, Consejo Superior de Investigaciones Científicas, c/Eduardo Cabello 6, 36208 Vigo, Spain*
[d] *Departamento de Física, Facultad de Ciencias del Mar,Universidad de Vigo, Apdo. 874, 36200 Vigo, Spain*
[e] *Departament de Física, Universitat de les Illes Balears, Spain*
[f] *Institut Mediterrani d'Estudis Avançats, IMEDEA (CSIC-UIB), Carretera de Valldemossa, km 7.5, 07071 Palma de Mallorca, Spain*
[g] *In. nova Oceanografia Litoral, c/Independència 361, ent. 3er, 08024 Barcelona, Spain*

Received 10 May 1999; received in revised form 16 January 2001; accepted 15 June 2001

Abstract

In the framework of the FRUELA project, two oceanographic surveys were conducted by R/V *Hespérides* in the eastern Bellingshausen Sea, western basin of the Bransfield Strait and Gerlache Strait area during December 1995 and January 1996. The main hydrographic structures of the study domain were the Southern Boundary of the ACC and the Bransfield Front. The characteristics and zonation of local water masses are discussed in terms of temperature, salinity, dissolved oxygen, nutrient and inorganic carbon concentrations. Concentration intervals for water mass labelling, on the basis of chemical parameters in addition to the common θ/S-based classification, are defined. Silicate seems to be a very good discriminator for local water masses.

1. Introduction

The Bransfield Strait is a semi-enclosed Antarctic sea located between the South Shetlands archipelago and the Antarctic Peninsula coast. The extent of the Strait is about 50,000 km^2 and it can be divided into three major basins which are separated from each other by sills shallower than 1000 m. The western basin of the Strait is connected to the neighbouring Bellingshausen Sea through passages existing between the westernmost South Shetland islands and also through the Gerlache Strait, and to the Drake Passage via the Boyd Strait principally. The Gerlache Strait is flanked by the western Antarctic Peninsula coast and the Palmer archipelago. The sill connecting the Gerlache Strait to the Bellingshausen Sea is about 350 m deep.

*Corresponding author. Current address: Direcció General de Ports i Transports, Generalitat de Catalunya, Av. Josep Tarradellas 2-6, 08029 Barcelona, Spain. Tel.: +34-93-495-8070; fax: +34-93-495-8196.

E-mail address: mgarlop@ciccp.es (M.A. García).

0967-0645/01/$ - see front matter
PII: S0967-0645(01)00113-8

In the framework of the FRUELA carbon flux study funded by the Spanish National Programme on Antarctic Research, two oceanographic surveys were conducted by R/V *Hespérides* in the eastern Bellingshausen Sea, western basin of the Bransfield Strait and Gerlache Strait area in December 1995 and in January 1996. From the point of view of physical oceanography, the aims of the surveys were to gain insight into the characterization of the local water masses including the details of their intraseasonal variability during Austral summer and to establish the local mesoscale circulation in the study region with a resolution which should be adequate to meet the project needs. This paper deals with the distribution of water masses as observed during the FRUELA 1995/96 cruises and the companion article by Gomis et al. (2002) discusses the 3D circulation and mass transport patterns.

The Bransfield Strait is one of the most densely observed Antarctic seas due to its geographical accessibility, its favourable sea ice conditions and the existence of multiple logistic resources in the area. Modern oceanographic research in the zone can be dated back to the Discovery expeditions in the late 20s (Clowes, 1934). The international ISOS and BIOMASS programmes, which were carried out during the late 70s and the early 80s respectively, produced a basic understanding of the local water mass structure and circulation patterns on the basis of coarse-resolution surveys (see e.g. Gordon and Nowlin, 1978; Grelowski et al., 1986; Tokarczyk, 1987). Hofmann et al. (1996) provided descriptions of the large scale water mass distribution and circulation patterns in the Bransfield Strait on the basis of historical hydrographic data.

A number of eddy-resolving field studies auspiced by the US and Spanish national Antarctic programmes targeted the mesoscale circulation at the different Bransfield Strait basins in the late 80s and early 90s (Niiler et al., 1991; García et al., 1994; López et al., 1994; López et al., 1999). In particular, Niiler et al. (1991) carried out a detailed analysis of the geostrophic circulation in the western Bransfield Strait region with a focus on the circulation variability at seasonal scale. Although Niiler et al.'s (1991) work provided a very useful reference for the oceanographic aspects of the FRUELA project, it was clear from the beginning that additional hydrographic observations of the area of interest should be a key component of the Spanish study. On one hand, the flow variability documented by Niiler et al. (1991) implied that ad hoc physical measurements were needed to compute fluxes of biogeochemical variables contemporary to data acquisition. On the other hand, Niiler et al. (1991) could not extend their measurements deeper than 200 m due to limitations of resources and shiptime imposed by the funding programme. This resulted in an underestimation of the magnitude of the major local circulation feature—the Bransfield Current—possibly by one half (Gomis et al., 2002). Given the presumed importance of the advective transport term in the local carbon budget (see Huntley et al., 1991), reassessing the geostrophic transport with a deeper reference layer was regarded as a must.

2. Material and methods

R/V *Hespérides* conducted two cruises in the FRUELA study area in December 1995 and in January 1996, respectively. The December 1995 cruise comprised two hydrographic legs. In leg 1 (hereafter referred to as MACRO '95), a series of 5 hydrographic transects were visited across the major hydrographic fronts of the project study area. This leg was carried out between 3rd and 11th December and was composed of 33 stations (Fig. 1a). The characteristic spacing between adjacent stations was about 17 nautical miles on each transect and the spacing between adjacent transects was twice as long. Leg 2 (named MESO '95 in what follows) consisted of a higher-resolution survey of the western Bransfield basin and the Gerlache Strait carried out between 12th and 19th December. In this leg, 107 hydrographic stations were visited and the typical spacing between adjacent stations was about 8 nautical miles. As for the January 1996 cruise, it included one single hydrographic leg (MACRO '96) which replicated the MACRO '95 survey except for the westernmost transect in the Bellingshausen Sea (Fig. 1b).

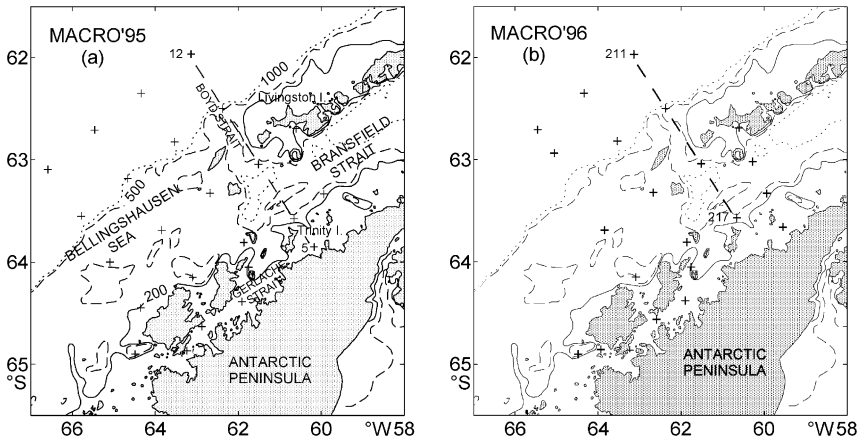

Fig. 1. (a) Map of hydrographic stations where water samples were obtained during the MACRO '95 leg, December 1995 cruise. (b) Same for the MACRO '96 leg, January 1996 cruise. The CTD station coverage of each survey is shown in Figs. 2a and 4a. The dashed straight lines indicate the locations of the vertical sections represented in Figs. 6 and 7. The 0-m, 200-m, 500-m and 1000-m depth contours are depicted.

Twenty seven stations were occupied in the MACRO '96 leg from 21st to 27th January 1996. During both MACRO '95 and MACRO '96, a section along the Gerlache Strait was sampled. As the main aim of this paper is to explore the intraseasonal variability of the local hydrography and to discuss concentration thresholds of the local water mass labelling, we shall only focus on the MACRO '95 and MACRO '96 data sets. Both sets and the MESO '95 data are used in the companion paper by Gomis et al. (2002) to compute the local 3D mesoscale circulation and related transports.

On each hydrographic station, a surface-to-bottom CTD cast was performed with a GO MkIIIC WOCE probe provided with extra dissolved oxygen, fluorescence and light transmission sensors. Water samples were obtained routinely at 24 levels with a GO Rosette equipped with 101 Niskin bottles. Some of the Niskin bottles carried RTM SiS 4002 digital reversible thermometers. Salinity was obtained from water samples by means of a Guildline Autosal 8600 B. Dissolved oxygen concentrations were measured following Winkler's method, with an estimated error of ± 1 μmol/kg. Nutrient concentrations were determined by segmented flow analysis with Technicon AAII autoanalyzers, following Hansen and Grasshoff (1983) with some improvements (Mouriño and Fraga, 1985; Álvarez-Salgado et al., 1992). Alkalinity and pH(NBS) were determined by potentiometric methods according to Pérez and Fraga (1987a, b). The accuracy of pH and alkalinity, estimated using CO_2 certified reference material, was ± 0.004 and ± 1.4 μmol/kg, respectively. Total inorganic carbon (TIC) concentrations were computed from pH and alkalinity data by using the thermodynamic equations of the carbonate system (Dickson, 1981) and the constants determined by Mehrbach et al. (1973) with an accuracy of ± 4 μmol/kg (Millero, 1995; Lee et al., 1996). TIC data were normalized at salinity 35 psu by means of the formalism NTIC = TIC*35/S. Water sample analyses were carried out on board.

The contouring package used to map the distributions is the Surface Mapping System v. 6.03 from Golden Software Inc. The θ and S distributions have been derived from CTD profiles whereas water sample data (available on every other CTD station) have been used for the spatial interpolation of chemical properties. The land areas have been masked after the interpolation, so details of the interpolated fields near coastal boundaries may not be properly assessed.

3. Local water masses and fronts

The water mass zonation of the FRUELA study area in terms of physical water properties is quite well established in the literature. A summary of the local water mass classification used follows for reference. The conventions are similar to those used by García et al. (1994), García (1996) and López et al. (1999), which were distilled from literature and were applied to analyses undertaken in the framework of previous Spanish Antarctic reserach projects. For the sake of clarity, the description has been splitted into three parts: (i) eastern Bellingshausen Sea and southern Drake Passage, (ii) Bransfield Strait and (iii) Gerlache Strait.

The typical water masses sequence in the eastern Bellingshausen Sea and southern Drake Passage sector consists of four main water masses: Antarctic Surface Water (AASW), Upper Circumpolar Deep Water (UCDW), Lower Circumpolar Deep Water (LCDW) and Antarctic Bottom Water (AABW). AASW is a cold water mass originated all around Antarctica in early winter and typically extending down to 200 m. The hydrographic signature of the AASW core is a subsurface temperature minimum (typically $\theta<0^{\circ}$C) embedded in a strong halocline. Below AASW, a two-layer system of Circumpolar Deep Water (CDW) occupies most of the water column. The difference in physical properties between both CDW cores, upper CDW (UCDW) and lower CDW (LCDW) corresponds to their different extra-Antarctic origin and is subtle. The deep $\theta = 0^{\circ}$C isoline is considered to be the boundary between LCDW and AABW. In the sector, AABW mostly consists of Weddell Sea Deep Water which is advected westward after leaving the Weddell basin through deep gaps across the South Scotia Ridge and also further east.

The Southern ACC Front (SACCF) and the Southern Boundary of the ACC (SbyACC) as they were defined by Orsi et al. (1995) are the main hydrographic features in the eastern Bellingshausen Sea and southern Drake Passage. The SACCF is the only ACC front that does not separate distinct water masses. In the FRUELA study domain, the SbyACC shows as a structure which separates the ACC waters from an area of relatively vertical hydrographic homogeneity extending on the South Shetlands continental shelf. In our case, the locus where the 0°C isotherm intersects the surface layer can be roughly considered as the position of the SbyACC. Eastward-flowing geostrophic jets are related to both the SACCF and the SbyACC in the southern Drake Passage, although the SbyACC jet is not a circumpolar feature like the SbyACC itself (the hydrographic expression of the SbyACC is not a density front everywhere).

From the hydrographic point of view, the Bransfield Strait is best defined as a transition zone between the Bellingshausen Sea and the Weddell Sea. The Strait basins are mostly occupied by water masses whose properties are controlled by the characteristics of the inflows from the adjacent seas—a warm and relatively fresh inflow from the Bellingshausen Sea (typically 0.5–3.0°C and 33.1–33.9 psu in summer) and a cool and relatively salty inflow of Weddell Sea surface and deep waters (typically with negative temperatures and salinity ranging from 34.1 to 34.6 psu in summer) -. The main local water masses can then be referred to as Transitional Zonal Waters with Bellingshausen Sea influence (TBW) and Transitional Zonal Waters with Weddell Sea influence (TWW) depending on the dominant source waters. Both water masses are separated by a shallow hydrographic front which has a clear surface thermal signature—several summer cruises performed in the area suggest that the 1.0°C isotherm is a good discriminator between TBW and TWW in mid summer. TBW appears confined to a narrow stretch of the mixed layer extending along the northern half of the Strait whereas TWW occupies almost the entire volume of the Bransfield basins. As mentioned before, modified LCDW may flow into the Bransfield Strait through the Boyd Strait and other passages. When it occurs, it replaces TWW and produces a characteristic deep temperature maximum ($\theta > 0^{\circ}$C). Still another water mass can be traced below the TWW layer—the Bransfield Deep Water (BDW). It is believed that this water mass is an isopycnal mixture of Weddell Sea shelf waters and Warm Deep Water which is advected into the eastern part

of the Bransfield Strait and may be further modified in situ by winter convection. The −1.0°C and 34.5 psu θ and salinity values define the shallowest extent limit of BDW under TWW.

Two hydrographic fronts have been described in the Bransfield Strait: the aforementioned TBW/TWW surface front and the so-called Bransfield Front (BF)—the density front extending along the southern South Shetlands continental slope, which separates TWW from waters sitting on the archipelago's shelf. Of the two, only the BF is relevant from the dynamical point of view. As both fronts occupied the same geographic position during the FRUELA cruises, the combined frontal zone will be referred to as BF.

The hydrography of the Gerlache Strait has been little discussed in the open literature, to the authors' knowledge. As a first approach, the Gerlache Strait can be understood as a westward extension of the western basin of the Bransfield Strait. Given the depth range of the Gerlache Strait and the shallow sill existing on its western end, no BDW should be present in the area. The typical Gerlache Strait water column should then consist of an upper layer of TBW and an underlying, bottom-reaching layer of TWW. Limited intermediate intrusions of CDW could be expected to penetrate either from the west or from the east. Local TBW should be fresher and cooler than in the Bransfield Strait due to the influence of freshwater inputs from local glaciers.

4. Results

4.1. Horizontal zonation

Figs. 2 and 3 show the horizontal distributions of θ, S, oxygen, nitrate, silicate and NTIC at sea surface and at 300 m depth in the western basin of the Bransfield Strait and eastern Bellingshausen Sea as deduced from the MACRO '95 data set. Figs. 4 and 5 show similar distributions for the MACRO '96 data.

The MACRO '95 leg was carried out in early December shortly after sea ice retreat in the Bransfield Strait. This is clearly noticeable in Figs. 2a and b, which display low sea surface temperature and salinity values with respect to the canonical local summer range of θ and S. Contrary to this, the sea surface distributions of temperature and salinity in late January 1996 (Figs. 4a and b) match better with the paradigm for local summer conditions—in our case, the BF front can be traced through the 34.0 psu isohaline. A comparable situation is found, e.g., when comparing data from the previous BRANSFIELD 9112 cruise carried out in December 1991 (Rojas et al., 1996) with the distributions of the BIOANTAR 93 cruise performed in January 1993 (García et al., 1994). A similar but less pronounced intraseasonal change of temperature—of about 0.2°C between December 1995 and January 1996—can be noticed in the 300 m distributions of θ in the southern half of the western Bransfield Strait. The signature of the BF is visible in both deep distributions of θ. The comparison of the temperature distributions suggests a limited variability of the BF between the two study periods. The deep horizontal salinity distributions show very little structure (Figs. 3b and 5b).

The sea surface distribution of oxygen for MACRO '95 shows a zone of high oxygen concentrations ($O_2 > 390$ μmol/kg) coinciding with low nitrate ($NO_3 < 20$ μmol/kg) and low NTIC (NTIC < 2150 μmol/kg) levels in the northeastern Bellingshausen Sea (Figs. 2c–e), in particular where a meandering jet associated with the SbyACC was observed (Gomis et al., 2002). Strong phytoplankton accumulation in this region caused this signal in the chemical field (Varela et al., 2002). No similar feature was observed during MACRO '96 one month later. In this second cruise, the highest oxygen ($O_2 > 380$ μmol/kg), lowest nitrate ($NO_3 < 16$ μmol/kg) and lowest NTIC (NTIC < 2170 μmol/kg) values were registered in the Gerlache Strait related to phytoplankton nutrient consumption/oxygen production—high chlorophyll concentrations were measured at these stations (see Varela et al., 2002; Álvarez et al. 2002; Castro et al., 2002). At 300 m depth, the distributions of the chemical properties clearly follow the thermohaline distributions and a high percentage of the chemical variability can be explained by variations in the thermohaline properties. No significant variability

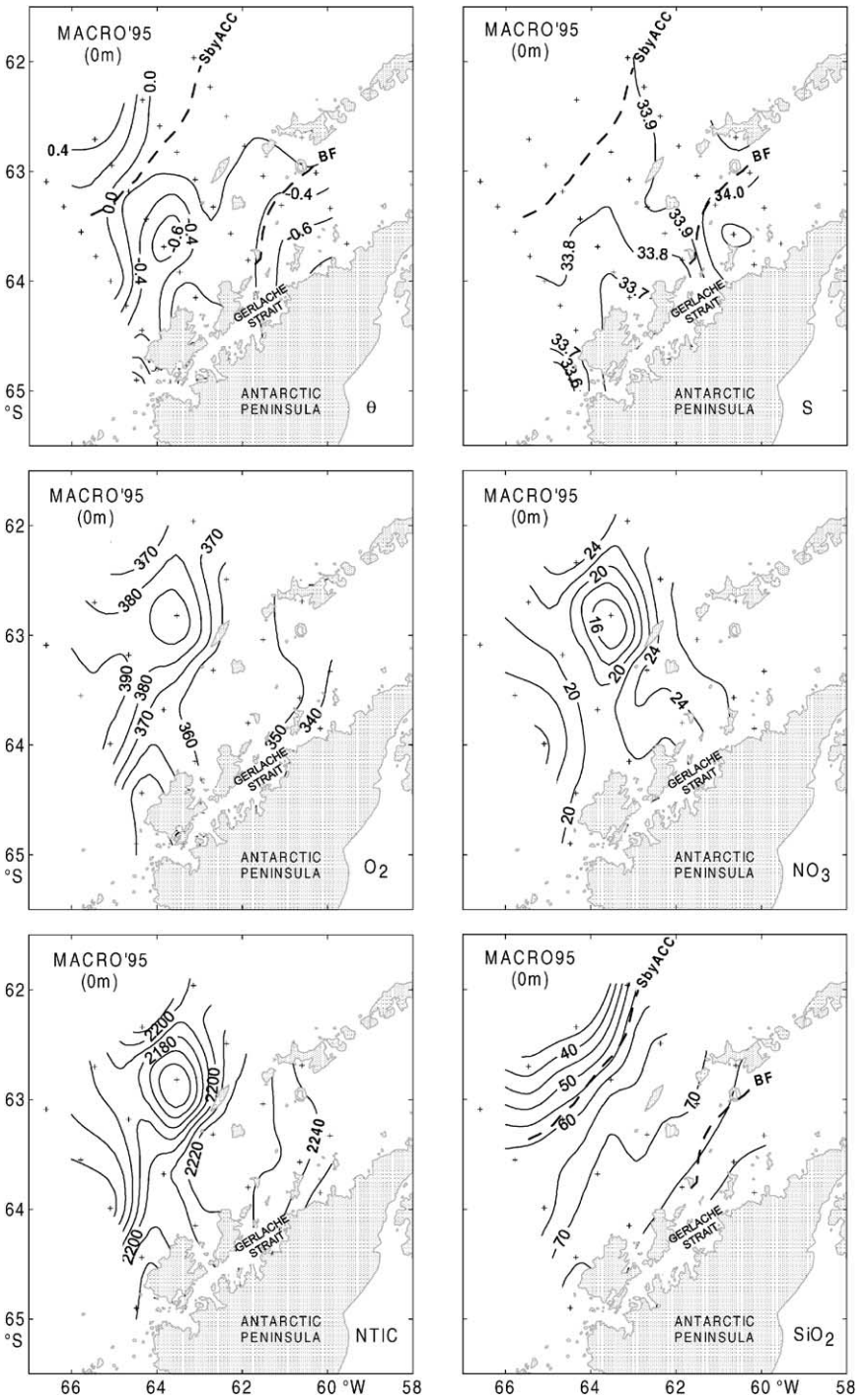

Fig. 2. MACRO '95 leg. Surface horizontal distributions of (a) potential temperature (°C), (b) S (psu), (c) O_2 (μmol/kg), (d) nitrate (μmol/kg), (e) NTIC ($=\mathrm{TIC}\cdot 35/S$; μmol/kg) and (f) silicate (μmol/kg) in the western basin of the Bransfield Strait and Bellingshausen Sea.

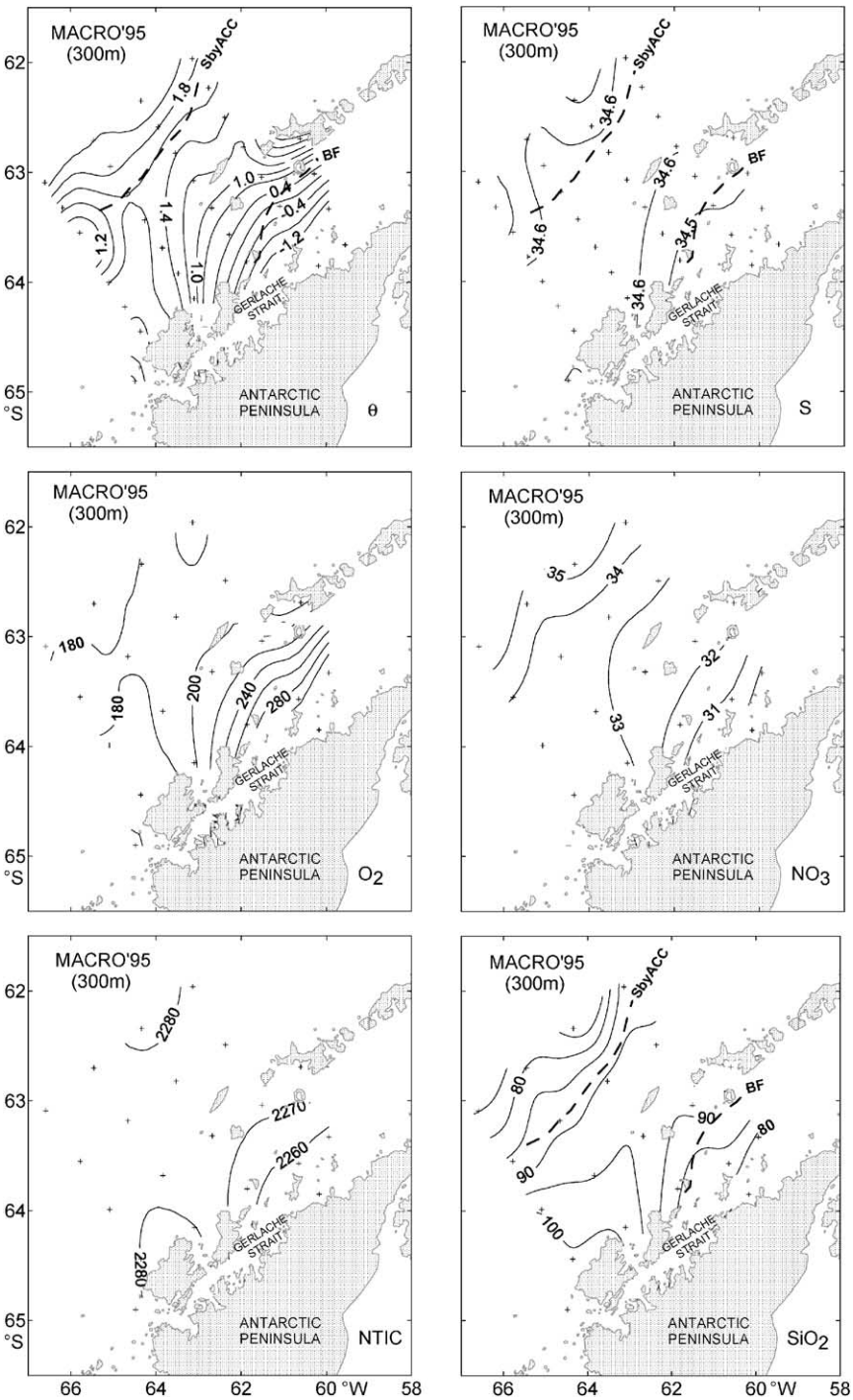

Fig. 3. MACRO '95 leg. Horizontal distributions at 300 m of (a) potential temperature (°C), (b) S (psu), (c) O_2 (μmol/kg), (d) nitrate (μmol/kg), (e) NTIC ($=\mathrm{TIC}\cdot 35/S$; μmol/kg) and (f) silicate (μmol/kg) in the western basin of the Bransfield Strait and Bellingshausen Sea.

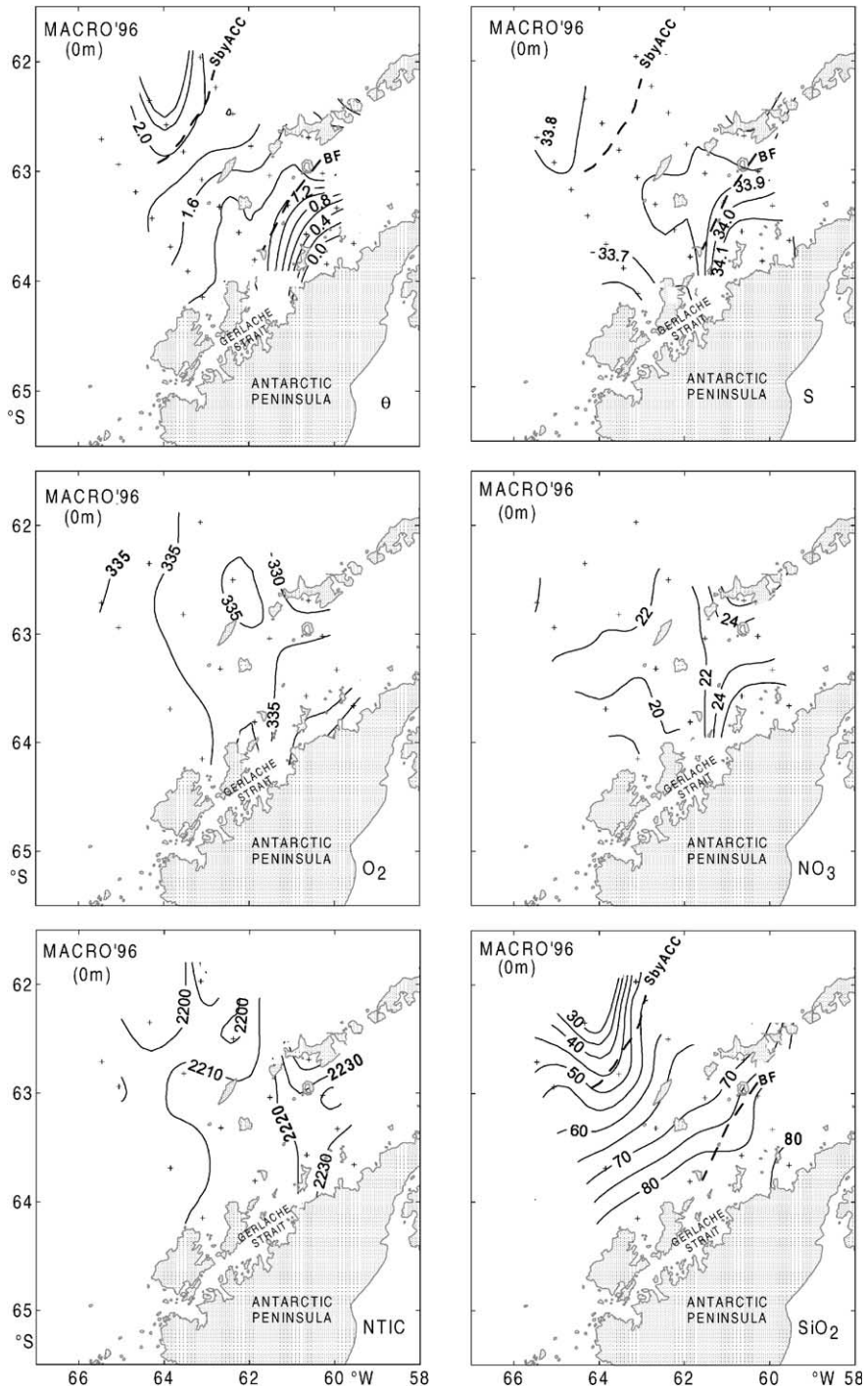

Fig. 4. MACRO '96 leg. Surface horizontal distributions of (a) potential temperature (°C), (b) *S* (psu), (c) O_2 (μmol/kg), (d) nitrate (μmol/kg), (e) NTIC (μmol/kg) and (f) silicate (μmol/kg) in the western basin of the Bransfield Strait and Bellingshausen Sea.

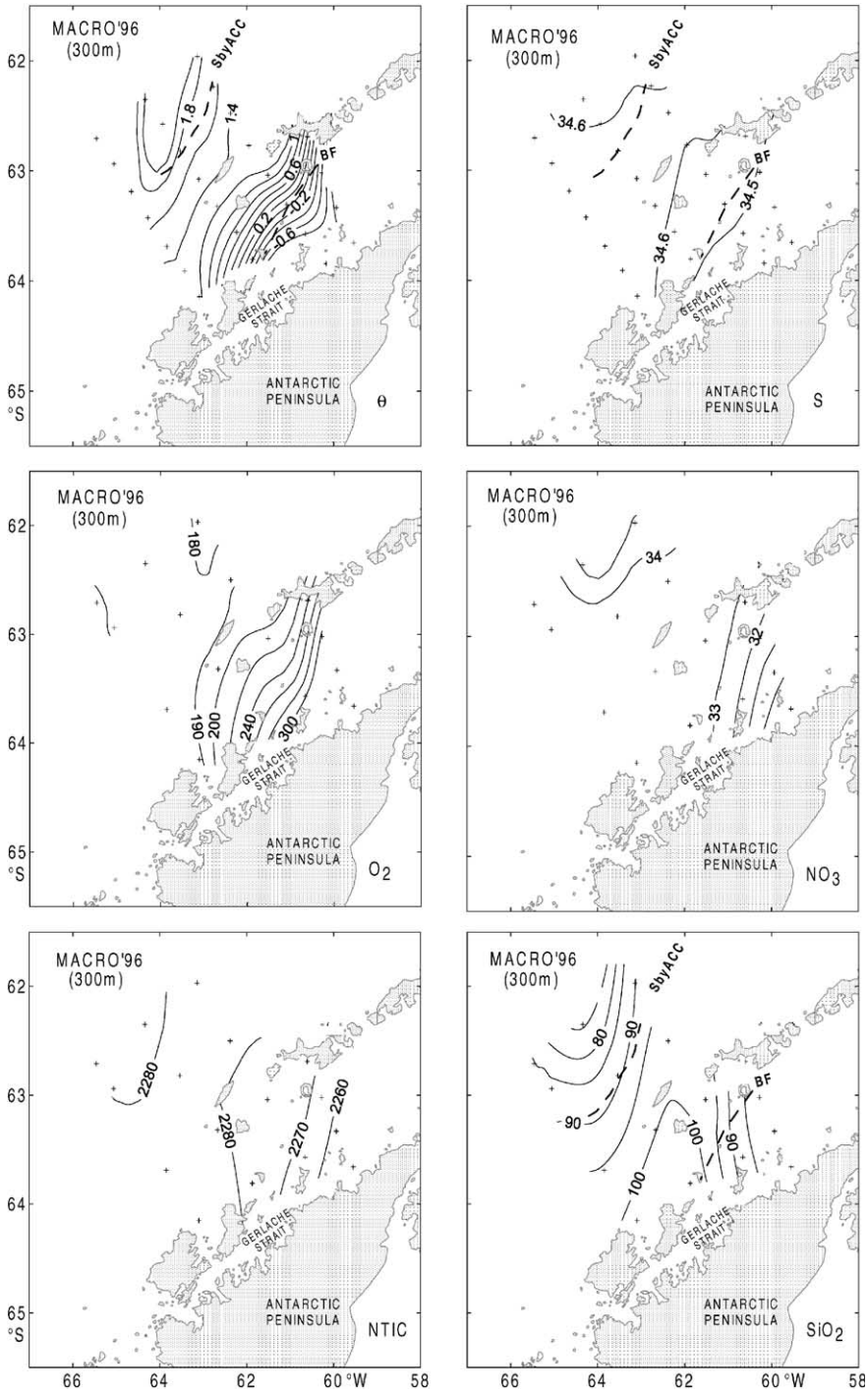

Fig. 5. MACRO '96 leg. Horizontal distributions at 300 m of (a) potential temperature (°C), (b) *S* (psu), (c) O_2 (μmol/kg), (d) nitrate (μmol/kg), (e) NTIC (μmol/kg) and (f) silicate (μmol/kg) in the western basin of the Bransfield Strait and Bellingshausen Sea.

was observed between the two surveys. The distributions of all the chemical properties (Figs. 3c–e, 5c–e), show strong gradients in the SbyACC and BF regions. The low oxygen ($O_2 < 180\,\mu mol/kg$), high nitrate ($NO_3 > 35\,\mu mol/kg$) levels north of the SbyACC reflect the southward extension of the LCDW. On the other hand, waters with Weddell Sea influence can be easily traced by high oxygen ($O_2 > 250\,\mu mol/kg$) and low nitrate ($NO_3 < 32\,\mu mol/kg$) and NTIC (NTIC $< 2270\,\mu mol/kg$) in the southeastern region of the Bransfield Strait.

The distributions of silicate behave in a more conservative way than the other chemical properties (i.e. nitrate distributions) in the study area. Figs. 2f and 4f show a consistent picture of the silicate distribution at sea surface which apparently is not affected by the December 1995 phytoplankton bloom nor by any other source of intraseasonal variability. The surface waters of the Bransfield Strait have silicate concentrations exceeding $65\,\mu mol/kg$ whereas the corresponding values are $< 60\,\mu mol/kg$ in the eastern Bellingshausen Sea. Moreover, the position of the SbyACC can be easily traced via the horizontal gradient of the sea surface silicate concentrations. This is not so clear, however, for the BF. The position of the SbyACC is also noticeable in the silicate distribution at 300 m depth, although at this level waters pertaining to the ACC region do not have significantly different silicate concentrations from Bransfield Strait waters.

4.2. Vertical distribution of water masses

Figs. 6 and 7 display the vertical distributions (up to 1200 m) of the thermohaline and chemical properties along the eastern Bellingshausen Sea–Bransfield Strait transect through the Boyd Strait corresponding to the MACRO '95 and MACRO '96 surveys. Despite the θ and the S distributions exhibit the same overall pattern in both legs, a closer view reveals two noteworthy differences (Figs. 6a and b, 7a and b). One is that sea surface temperature and salinity of the MACRO '95 leg are lower—by roughly 1°C and 0.1 psu, respectively—than in the MACRO '96 leg (Figs. 2a and b, 4a and b), which is a clear signal of hydrographic intraseasonal variability in the study area (the MACRO '95 θ and S values were influenced by melting of the sea ice cover occurred shortly before the cruise whereas the MACRO '96 distributions display full summer conditions). On the other hand, the intrusion of modified LCDW into the Bransfield Strait was larger in January 1996 than in December 1995, as the temperature distribuions reveal (see Figs. 6a and 7a). Moreover, a careful scrutiny of the details of the θ distributions shows that this feature is not an interpolation artifact—the area covered by the 1.0°C isotherm does not include any of the data points of station 8 in the MACRO '95 distribution shown in Fig. 6a, whereas it includes all points below 300 m in the corresponding station (stn 215) of the MACRO '96 distribution depicted in Fig. 7a. We think that differential intrusion of CDW is related to undersampled deep mesoscale variability of the LCDW inflow—García et al. (1994) reported time series observations of temperature at 400 m acquired south of Deception Island during Austral summer 1992/93 which displayed transient temperature increases which could only be explained by variability of the intrusion of CDW at mesoscale. On the other hand, there was no signature of BDW on the transect in any of the two occupations during the FRUELA study.

As in the horizontal distributions shown before, the vertical distributions of oxygen, nitrate and NTIC (Figs. 6c–e, 7c–e) closely mirror the temperature distributions. However, the temperature minimum of AASW, at about 80 m depth, is not traced in the chemical fields. At this depth, strong gradients are observed in the chemical properties. Below AASW, the poleward extension of CDW is clearly discerned by minimum oxygen values and maximum concentrations of nitrate and NTIC. However, the chemical properties extrema are not located at the same depth. For the two cruises, we found the nitrate and NTIC maxima at about 250 m depth and the oxygen minimum a little deeper (~ 350 m depth). In addition, the differential intrusion of CDW into the Bransfield Strait is also evident in these vertical distributions. During MACRO '96, lower oxygen ($O_2 < 200\,\mu mol/kg$), higher nitrate ($NO_3 > 33\,\mu mol/kg$) and higher NTIC (NTIC $> 2280\,\mu mol/kg$) values were reached

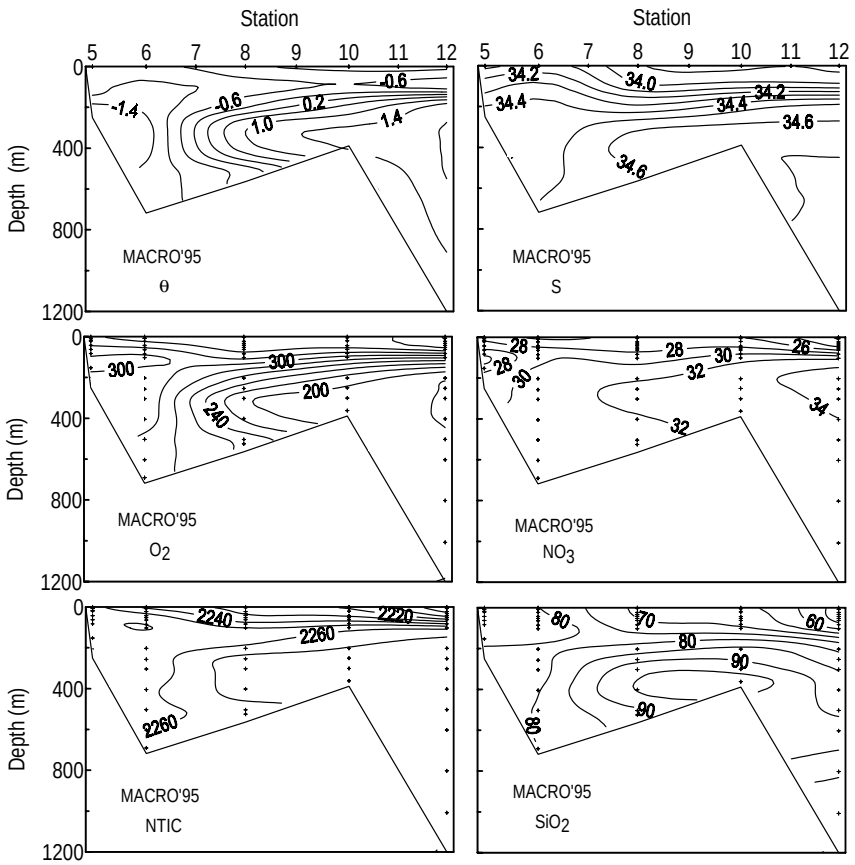

Fig. 6. MACRO '95 leg. Vertical distributions of (a) potential temperature (°C), (b) *S* (psu), (c) O_2 (μmol/kg), (d) nitrate (μmol/kg), (e) NTIC (μmol/kg) and (f) silicate (μmol/kg) along the Bellingshausen Sea–Bransfield Strait transect through the Boyd Strait. The Drake Passage is on the right and the Bransfield Strait is on the left.

at stn 215 in comparison with concentrations measured at stn 8 during the December 1995 cruise. On the other hand, the strong vertical chemical gradients between stns 6–8 for MACRO '95 and stns 217–215 for MACRO '96 mark the position of the BF closely following the temperature distributions (Figs. 6a and 7a). South of the front, the domain of Weddell Sea water influence is defined by high oxygen ($O_2 > 280$ μmol/kg), low nitrate ($NO_3 < 32$ μmol/kg) and low NTIC (NTIC < 2260 μmol/kg) levels.

As regards to silicate, it is seen again to be a better tracer of local water masses than nitrate (Figs. 6f and 7f). This is indeed clear in the upper 100 m, where the MACRO '95 and MACRO '96 vertical distributions of silicate are very similar. At depth, the maximum silicate concentration values were attained just south of the Boyd Strait during both cruises. This fact and the shape of the silicate concentration isolines suggest that these maxima were related to the inflow of LCDW into the Bransfield Strait. With respect to this, the increase of the deep silicate concentrations in about 10 μmol/kg between December 1995 and January 1996 would be an expression of larger LCDW inflow.

Figs. 8 and 9 depict interpolated vertical distributions of potential temperature, salinity, oxygen, nitrate, NTIC and silicate along the Gerlache Strait obtained from the MACRO '95 and

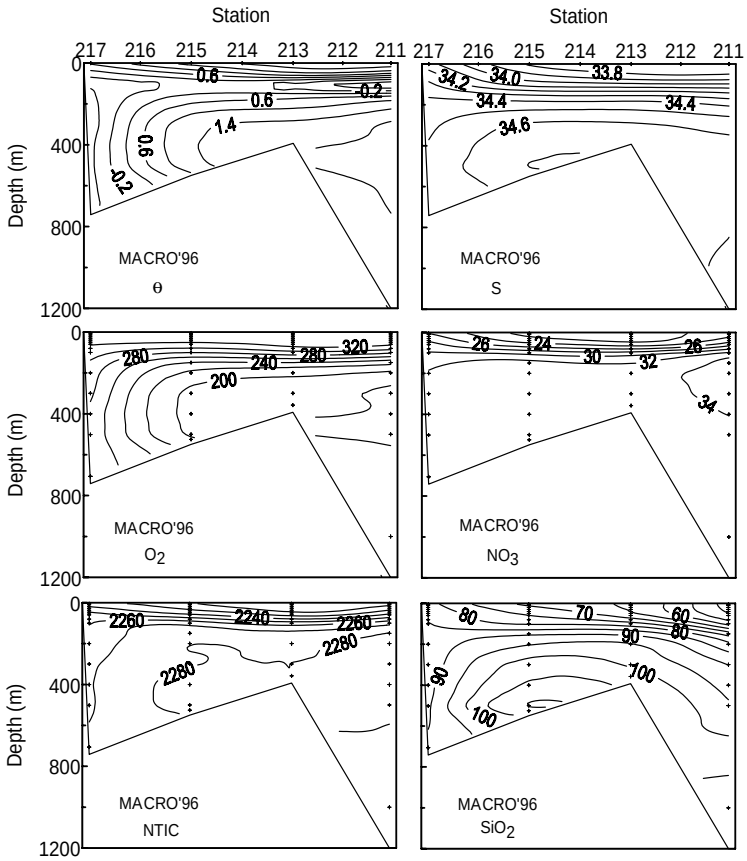

Fig. 7. MACRO '96 leg. Vertical distributions of (a) potential temperature (°C), (b) *S* (psu), (c) O_2 (μmol/kg), (d) nitrate (μmol/kg), (e) NTIC (μmol/kg) and (f) silicate (μmol/kg) along the Bellingshausen Sea–Bransfield Strait transect through the Boyd Strait. The Drake Passage is on the right and the Bransfield Strait is on the left.

MACRO '96 data sets. The θ and S sections (Figs. 8a and b, 9a and b) show a consistent pattern whose overall features are repeated in both legs. The vertical distributions of temperature (Figs. 8a and 9a) are similar to that obtained by Roese and Speroni (1995) using XBTs in February 1991. The water sequence west of the Bismarck Strait—i.e., the western end of the Gerlache Strait—consists of a surface layer of AASW including a temperature minimum and a deep layer of CDW which hosts both the temperature and the salinity maxima. In the eastern Bellingshausen Sea, UCDW reaches the shelf break and is observed near 300 m (Klinck, pers. comm.). It may be that LCDW has risen to 300 m northwest of the Bransfield Strait as the ACC (and UCDW) shifts offshore. If this was the case during the FRUELA cruises, CDW flowing from the Bellingshausen Sea into the Gerlache Strait would be LCDW. But it might also be that the CDW entering the Gerlache Strait is uplifted UCDW. In any case, the warm water found in the Gerlache Strait at depth is certainly some sort of CDW modified through heat exchange with the surface and mixing with coastal waters.

Water flows from the Bellingshausen Sea into the Gerlache Strait through multiple paths like via Bismarck Strait and through Dallman Bay and the Scholaert Channel (Klinck, pers. comm.). The Bellingshausen Sea inflow has to pass over sills

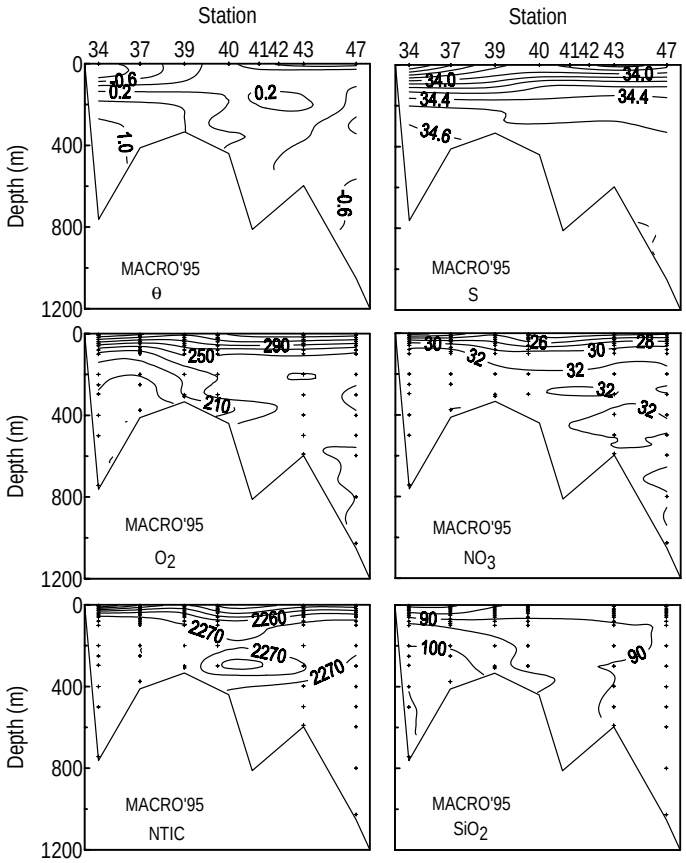

Fig. 8. MACRO '95 leg. Vertical distributions of (a) potential temperature (°C), (b) *S* (psu), (c) O_2 (μmol/kg), (d) nitrate (μmol/kg), (e) NTIC (μmol/kg) and (f) silicate (μmol/kg) along the Gerlache Strait. The Bellingshausen Sea is on the left and the Bransfield Strait is on the right.

whose depths are less than 400 m and this places an important constraint to CDW. Most of the CDW layer is "lost" and is replaced by TWW to the extent that the deep temperature maximum which characterizes CDW is totally eroded at the centre of the Gerlache Strait. At surface, a sharper transition from AASW to TBW is observed. As expected, TBW in the Gerlache Strait is somewhat cooler and fresher than in the Bransfield Strait. Back to deep layers, an isolated temperature maximum ($\theta > 0.2$°C) is observed near the eastern end of the Gerlache Strait at depths of the order of 200 m. Given the fact that the salinity corresponding to this maximum is lower than the salinity of the CDW core in the western part of the Strait, its oxygen concentration is higher and its silicate levels are lower, and also taking the local bathymetric setting of the Gerlache Strait and surroundings into account, we believe that this feature may correspond to a filament of modified CDW advected from the western Bransfield basin. Another possible explanation is that this water body consists of Bellingshausen Sea CDW flown into the Gerlache Strait through the Scholaert Channel or other passage further east. The differences in properties with respect to CDW found in the western part of the Gerlache Strait would then result from mixing with waters adjacent to the western flanks of the Strait.

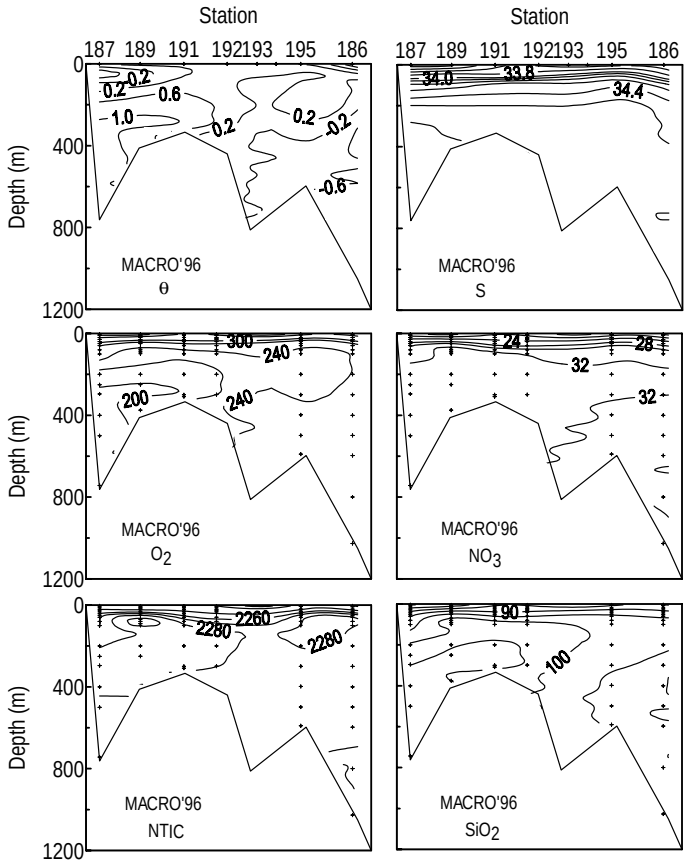

Fig. 9. MACRO '96 leg. Vertical distributions of (a) potential temperature (°C), (b) *S* (psu), (c) O_2 (μmol/kg), (d) nitrate (μmol/kg), (e) NTIC (μmol/kg) and (f) silicate (μmol/kg) along the Gerlache Strait. The Bellingshausen Sea is on the left and the Bransfield Strait is on the right.

The only remarkable differences between the MACRO '95 and MACRO '96 θ and *S* distributions along the Gerlache Strait are constrained to the upper layers. As was the case in the western basin of the Bransfield Strait, the MACRO '96 sea surface temperatures were higher in the Gerlache Strait than the corresponding MACRO '95 values (see Figs. 8a and 9a) due to seasonal warming, but unlike in the Bransfield, the surface salinity was lower in January 1996 than in December 1995. This probably reflects the increase of the freshwater supply related to melting processes at local glaciers and passing icebergs as Austral summer progresses. In a limited-area basin as the Gerlache Strait, such freshwater inputs must have a significant effect on surface water properties.

The distributions of oxygen, nitrate and NTIC along the Gerlache for the two cruises are strongly determined by phytoplankton consumption in the upper meters of the water column. High oxygen concentrations, low nitrate and low NTIC values were obtained on both sides of the Gerlache Strait due to local high phytoplankton accumulation (Varela et al., 2002; Álvarez et al., 2002; Castro et al., 2002). In fact, the lowest nitrate (NO_3 $<12\,\mu mol/kg$) and NTIC (NTIC $<2195\,\mu mol/kg$) concentrations for the two surveys were registered near the southwestern end of the Gerlache Strait during MACRO' 96. In the central sector of the

Gerlache Strait, a deep mixed layer probably prevented phytoplankton accumulation (Castro et al., 2002) and consequently lower oxygen and higher nitrate and NTIC levels were observed.

The vertical distributions of oxygen, nitrate and NTIC in the Gerlache Strait precisely mimic the temperature distributions at layers deeper than 100 m (Figs. 8c–e, 9c–e). The deep oxygen minimum ($O_2 < 220\,\mu mol/kg$), nitrate maximum ($NO_3 > 32\,\mu mol/kg$) and NTIC maximum ($NTIC > 2280\,\mu mol/kg$) are related to the above cited inflows of LCDW. Again as in the Bransfield Strait and in the eastern Bellingshausen Sea, silicate seems to be a good tracer of LCDW (see Figs. 8f and 9f). The silicate concentration range within the LCDW body in the Gerlache Strait matches the values displayed by LCDW in the rest of the FRUELA study area.

5. Discussion

In Table 1, we show the average values of the thermohaline and chemical properties for the different water masses sampled in the study area. In the eastern Bellingshausen Sea, the presence of AASW is clearly noticeable through the temperature minimum at about 80 m depth. The average thermohaline properties of this minimum were warmer and saltier during the MACRO' 96 due to intraseasonal variability (Table 1). The average concentrations of oxygen, nitrate and NTIC were not very different between the two cruises and no correlation with the thermohaline properties was found. However, about 52% and 68% of the observed variability of silicate concentration in the MACRO '95 and MACRO '96 data sets, respectively, can be explained by temperature and salinity. Whitehouse et al. (1995), using data from a transect sampled in the Belllingshausen Sea west of our study area during the UK STERNA project, showed that silicate concentration in the core of AASW was determined by the hydrographic variability in contrast with nitrate, which presented an homogeneous distribution.

North of the SbyACC, we can distinguish the cores of UCDW and LCDW in the chemical field. The UCDW maximum temperature is associated to an oxygen minimum and both nitrate and NTIC maxima (Table 1). UCDW's average temperature in the area of the Bellingshausen Sea sampled by R/V *Hespérides* was higher during MACRO '95 than in MACRO '96 whereas LCDW presented the highest average temperatures in MACRO '96. The temperature changes in the UCDW and LCDW cores were correlated to the changing levels of nitrate. On the other hand, strong gradients in sea surface silicate distributions were observed across the SbyACC in the two surveys. Veth et al. (1997) also described a strong silicate surface gradient associated with this structure at 6°W.

In the southwestern part of the Gerlache Strait, we found similar thermohaline and chemical properties of AASW for the two cruises (Table 1). AASW in the Gerlache Strait was less saline than at the eastern Bellingshausen Sea. Also during the two cruises, the layer of LCDW presented lower temperature and salinity values with respect to the Bellingshausen Sea. Dilution of the LCDW signal was also observed in oxygen, probably due to mixing with highly oxygenated TWW. However, nitrate and NTIC levels were not significantly different from the concentrations found in the Bellingshausen area and silicate levels were even higher, which might be a product of sediments supplied by local glaciers. In the northeast part of the Gerlache Strait, the water column was occupied by TBW over TWW, though a little intrusion of LCDW was registered. Regarding TBW, we found similar thermohaline properties for the two FRUELA cruises. Oxygen, nitrate and NTIC levels were influenced by phytoplankton consumption, being stronger during the MACRO '96 survey. However, silicate was not affected by phytoplankton activity as the region was dominated by *Cryptomonas* populations (Varela et al., 2002). In fact, silicate levels were very similar for the two cruises and higher than silicate concentrations for TBW in the western Bransfield region. TWW was found between 300–700 m depth in the Gerlache Strait, while in the Bransfield Strait it encompasses the whole water column at some areas—in particular, on the Antarctic Peninsula continental shelf. Consequently, we cannot

Table 1
Average and standard deviation of the thermohaline and chemical properties for the different waters masses found in the eastern Bellingshausen Sea (EBELLINGS), the Gerlache Strait (GERLACHE) and the western Bransfield Strait (BRANSFIELD) during the MACRO '95 and MACRO '96 surveys. We also have introduced the maximum and minimum values in the western Bransfield region during the MACRO'96 for comparison with Tokarczyk's water masses classification (see text and Table 2)[a]

Area	WT	θ	S	O_2	NO_3	SiO_2	NTIC
MACRO '95							
EBELLINGS	AASW	−0.94±0.24	33.97±0.05	309±16	29±1	66±11	2253±9
	UCDW	2.15±0.06	34.55±0.06	180±4	35.1±0.4	77±3	2279±4
	LCDW	1.6±0.2	34.69±0.02	188±7	32.9±0.3	97±6	2272±3
BRANSFIELD	TBW	−0.38±0.25	33.95±0.05	343±11	27±1	72±2	2239±10
	TWW	−0.80±0.15	34.18±0.08	330±16	27±1	81±2	2249±8
	LCDW	0.57±0.41	34.51±0.11	228±17	32.4±0.3	92±3	2273±1
GERLACHE	AASW	−0.68±0.47	33.92±0.07	278±2	29±1	88.2±0.2	2262±2
	CDW	0.96±0.30	34.57±0.07	195±13	32.9±0.1	102±3	2276±4
	TBW	0.44±0.53	33.88±0.13	321±24	26±2	87±1	2247±14
	TWW	−0.56±0.19	34.54±0.02	251±4	31.84±0.06	87±1	2266±2
MACRO '96							
EBELLINGS	AASW	−0.69±0.40	34.02±0.08	292±21	29±1	68±14	2258±12
	UCDW	2.07±0.04	34.635±0.003	175±1	34.2±0.1	87±5	2285±1
	LCDW	1.82±0.17	34.66±0.02	181±4	33.2±0.5	90±6	2280±3
BRANSFIELD	TBW	0.84±0.51	33.93±0.11	322±11	25±2	75±6	2240±14
	TBW max	1.65	34.16	335	29.0	84	2268
	TBW min	0.02	33.72	291	21.3	68	2214
	TWW	−0.3±0.5	34.28±0.13	318±22	29±2	83±4	2252±12
	TWW max	0.66	34.53	351	32.7	91	2273
	TWW min	−0.92	34.08	271	25.2	76	2222
	LCDW	0.63±0.45	34.48±0.16	226±23	33.1±0.4	94±10	2279±2
	LCDW max	1.15	34.66	261	33.7	107.1	2283
	LCDW min	0.02	34.27	203	32.4	81	2275
GERLACHE	AASW	−0.71±0.21	33.79±0.01	285±12	29.4±0.6	91±4	2272±3
	CDW	1.15±0.20	34.61±0.06	195±8	33.4±0.2	107±2	2281±4
	TBW	0.47±0.19	33.71±0.25	328±47	20±6	86±6	2217±39
	TWW	−0.35±0.07	34.54±0.01	252±3	31.8±0.3	94±2	2276±2

[a] θ in °C, salinity (S) in psu and chemical property concentrations in μmol/kg. WT: water type.

directly compare the average property values from the two regions.

In the Bransfield Strait, the average temperature values for the upper water masses, i.e. TBW and TWW, reflect the seasonal heating (Table 1). For the two water masses, the low oxygen values for MACRO '96, associated with no significant changes in nitrate and NTIC concentrations between the two cruises, suggest the influence of remineralization processes during MACRO '96. During the two surveys, TBW was characterized by lower silicate values than TWW. The average temperature for LCDW was higher during MACRO '96, which we intrepret as the expression of a larger intrusion of this water mass in January 1996. Also the higher nutrient levels and lower oxygen values support this idea.

To our knowledge, the paper by Tokarczyk (1987) is the only paper published in the open literature in which an objective classification of water masses has been proposed for the Bransfield Strait on the basis of a statistical multidimensional analysis method involving both physical and chemical water properties. This author suggested a classification of Bransfield Strait waters in six groups to which the four local water masses discussed in Section 3 roughly correspond—TBW approximately corresponds to Tokarczyk's water

Table 2
Range of values of water properties measured during the FIBEX cruise, February–March 1981 (after Tokarczyk, 1987)[a,b]

Type	θ	S	O_2	NO_3	SiO_2	NTIC
1a	0.5–3.3	33.1–33.9	322–357	9–25	2–26	n.d.
1	0.1–0.8	32.9–33.9	327–379	2–16	20–60	n.d.
3	0.9–2.1	34.3–34.8	174–244	22–27	24–102	n.d.
4a	−1.3–1.5	33.6–34.4	261–353	10–24	11–73	n.d.
4b	−1.5–1.0	33.8–34.6	218–335	13–26	39–100	n.d.

[a] *Note*: Correspondence between water types from Tables 1 and 2: TBW ~ 1, 1a; TWW ~ 4a, 4b; LCDW ~ 3; BDW included in 4b. See text for more details.
[b] θ in °C, salinity (S) in psu, O_2 in μmol/kg, NO_3 in μmol/kg, SiO_2 in μmol/kg and NTIC in μmol/kg.

types 1 and 1a; TWW involves Tokarczyk's types 4a and 4b; modified LCDW is Tokarczyk's water type 3; BDW was not individualized by Tokarczyk but included in type 4b.

Table 1 shows the range of values of water properties measured in the western Bransfield Strait and Gerlache Strait during the MACRO '96 cruise and Table 2 displays equivalent values obtained by Tokarczyk for his water classes using the FIBEX 1981 data set (FIBEX 1981 was one of the cruises auspiced by the international BIOMASS programme and roughly covered the same study area as the FRUELA cruises in February–March 1981. Here we use the MACRO '96 data set for comparison because it was obtained under seasonal conditions which are closest to those of FIBEX 1981). The comparison of both tables suggests that Tokarczyk's (1987) water types are excessively broad in hydrographic terms. They are best discriminated in $\theta - S$ space but the ranges for oxygen, nitrate and silicate are too wide and overlap, so assigment of water samples to a particular water type on the basis of a single chemical property does not seem feasible. On the contrary, Bransfield Strait local water masses defined according to the conventions exposed in Section 3 do have the same distinct character in $\theta - S$ space but have much narrower ranges of chemical properties and little intersection among them.

Table 1 suggests that silicate is a very good discriminator of water masses in the Bransfield Strait. Moreover, the distributions shown in Figs. 8f and 9f evidence that silicate concentration has very little variability (at least, on a sub-seasonal scale), so it is a robust water mass indicator in the Gerlache Strait area. No interval can be assessed for BDW as it was not found in our study area. Another choice would be labelling water masses by using oxygen and nitrate concentrations jointly, but it has the obvious drawback that values in the euphotic zone are modified by non-physical causes.

Acknowledgements

We acknowledge the help and the support of the crew of R/V *Hesperides* and of all colleagues who made possible data acquisition during the FRUELA December 1995 and January 1996 cruises. We are specially grateful to Julia Figa, Manuel González, Joan Puigdefàbregas, Maribel Lloret, Pilar Rojas, Mario Manríquez, Marcel. lí Farrán, Jorge Guillén and Pere Masqué (hope to meet on board again!). Our special thanks to T. Rellán and M.V. González for the oxygen and CO_2 analyses during the two cruises and to M.J. Pazó for the nutrient analyses during the MACRO '96 cruise. This study has been funded by the Spanish Comisión Interministerial de Ciencia y Tecnologia, contract no. ANT94-1010.

References

Álvarez, M., Ríos, A.F., Rosón, G., 2002. Spatio-temporal variability of air-sea fluxes of carbon dioxide and oxygen in the Bransfield and Gerlache Straits during Austral summer 1995–96. Deep-Sea Research II 49, 643–662.

Álvarez-Salgado, X.A., Fraga, F., Pérez, F.F., 1992. Determination of nutrient salts by automatic methods both in seawater and brackish waters: the phosphate blank. Marine Chemistry 39, 311–319.

Castro, C.G., Ríos, A.F., Doval, M.D., Pérez, F.F., 2002. Nutrient utilisation and chlorophyll distribution in the Atlantic sector of the Southern Ocean during Austral summer 1995–96. Deep-Sea Research II 49, 623–641.

Clowes, A.J., 1934. Hydrology of the Bransfield Strait. Discovery Reports 9, 1–64.

Dickson, A.G., 1981. An exact definition of total alkalinity and procedure for the estimation of alkalinity and total inorganic carbon from titration data. Deep-Sea Research I 28 (6), 609–623.

García, M.A., 1996. BIO *Hesperides* covered WOCE SR1b in February 1995. International WOCE Newsletter 23, 33–35.

García, M.A., López, O., Sospedra, J., Espino, M., Gràcia, V., Morrison, G., Rojas, P., Figa, J., Puigdefàbregas, J., S.-Arcilla, A., 1994. Mesoscale variability in the Bransfield Strait region (Antarctica) during Austral summer. Annales Geophysicae 12 (9), 856–867.

Gomis, D., García, M.A., López, O., Pascual, A., 2002. Quasi-geostrophic 3D circulation and mass transport in the western sector of the South Sheltland Islands. Deep-Sea Research II 49, 603–621.

Gordon, A.L., Nowlin, W.D., 1978. The basin waters of the Bransfield Strait. Journal of Physical Oceanography 8, 258–264.

Grelowski, A., Majewicz, A., Pastuszak, M., 1986. Mesoscale hydrodynamic processes in the region of the Bransfield Strait and the southern part of Drake Passage during BIOMASS-SIBEX 1983/84. Polish Polar Research 7, 353–369.

Hansen, H.P., Grasshoff, K., 1983. Automated chemical analysis. In: K. Grasshoff, M. Ehrhardt, K. Kremlig (Eds.), Methods of Seawater Analysis. Verlag Chemie, Weinheim, 419pp.

Hofmann, E.E., Klinck, J.M., Lascara, C.M., Smith, D.A., 1996. Water mass distribution and circulation west of the Antarctic Peninsula and including Bransfield Strait. In: R.M. Ross et al. (Ed.), Foundations for Ecological Research west of the Antarctic Peninsula, Vol. 70, Antarctic Research Series, pp. 61–80.

Huntley, M., Karl, D.M., Niiler, P., Holm-Hansen, O., 1991. Research on Antarctic Coastal Ecosystem rates (RACER): and interdisciplinary field experiment. Deep-Sea Research II 38, 911–941.

Lee, K., Millero, F.J., Campbell, D.M., 1996. The reliability of the thermodynamic constants for the dissociation of carbonic acid in seawater. Marine Chemistry 55, 233–245.

López, O., García, M.A., S.-Arcilla, A., 1994. Tidal and residual currents in the Bransfield Strait, Antarctica. Annales Geophysicae 12 (9), 887–902.

López, O., Garcia, M.A., Gomis, D., Rojas, P., Sospedra, J., S.-Arcilla, A., 1999. Hydrographic and hydrodynamic characteristics of the eastern basin of the Bransfield Strait (Antarctica). Deep-Sea Research I 46, 1755–1778.

Mehrbach, C., Culberson, C.H., Hawley, J.E., Pytkowicz, R.M., 1973. Measurements of the apparent dissociation constant of carbonic acid in seawater at atmospheric pressure. Limnology and Oceanograhy 18, 897–907.

Millero, F.J., 1995. Thermodynamics of the carbon dioxide system in the oceans. Geochimica et Cosmochimica Acta 59, 661–677.

Mouriño, C., Fraga, F., 1985. Determinacion de nitratos en agua de mar. Investigacion Pesquera 49, 81–96.

Niiler, P., Amos, A., Hu, J.-H., 1991. Water masses and 200 m relative geostrophic circulation in the western Bransfield Strait region. Deep-Sea Research II 38, 943–959.

Orsi, A.H., Whitworth III, T., Nowlin Jr., W.D., 1995. On the meridional extent and fronts of the Antarctic Circumpolar Current. Deep-Sea Research I 42, 641–673.

Pérez, F.F., Fraga, F., 1987a. A precise and rapid analytical procedure for alkaliniy determination. Marine Chemistry 21, 169–182.

Pérez, F.F., Fraga, F., 1987b. The pH measurements in seawater on NBS scale. Marine Chemistry 21, 315–327.

Roese, M., Speroni, J., 1995. Dinámica de las aguas en Bahia Paraíso y su vinculación con el Estrecho de Gerlache, Antártida. Instituto Antartico Argentino, contribucion No. 416, 1–29.

Rojas, P., López, O., García, M.A., Arístegui, J., Torres, S., Hernández-León, S., Bastarrechea, G., Amengual, B., Escánez, J., Morales-Nin, B., 1996. Hidrografía del Estrecho de Bransfield durante el verano Austral 91/92. Actas del V Simposio Español de Estudios Antárticos, 403–411.

Tokarczyk, R., 1987. Classification of water masses in the Bransfield Strait and southern part of the Drake passage using a method of statistical multidimensional analysis. Polish Polar Research 41, 629–641.

Varela, M., Fernandez, E., Serret, P., 2002. Size-fractioned phytoplankton biomass and primary production in the Gerlache and south Bransfield Straits (Antarctic Peninsula) in Austral summer 1995–1996. Deep-Sea Research II 49, 749–768.

Veth, C., Peeken, I., Scharek, R., 1997. Physical anatomy of fronts and surface waters in the ACC near the 6W meridian during Austral spring 1992. Deep-Sea Research II 44, 23–50.

Whitehouse, M.J., Priddle, J., Woodward, E.M.S., 1995. Spatial variability of inorganic nutrients in the marginal ice zone of the Bellingshausen Sea during the Austral spring. Deep-Sea Research II 42, 1047–1058.